Studies of Boundary-Layer Cloud Field Anisotropy for Radiative Transfer

L. M. Hinkelman and E. E. Clothiaux
Department of Meteorology
Pennsylvania State University
University Park, Pennsylvania

K. F. Evans
Atmospheric and Oceanic Sciences
University of Colorado
Boulder, Colorado

T. P. Ackerman
Environmental and Health Sciences Division
Pacific Northwest National Laboratory
Richland, Washington

Introduction

Radiative transfer and heating in the cloudy atmosphere depend on the specific three-dimensional (3D) structure of the cloud field in question. However, detailed 3D cloud field measurements are rare. As a result, studies of 3D radiative transfer through clouds have frequently assumed that the spatial characteristics of cloud fields are isotropic in the horizontal dimensions. To investigate the validity of this assumption, the spatial characteristics of boundary-layer cloud fields produced by a large eddy simulation under various forcing conditions have been analyzed. The degree of anisotropy present in the cloud fields has been calculated and related to the meteorological conditions that influenced cloud development. Study of the interaction between solar radiation and the simulated cloud fields using Monte Carlo radiative transfer computations is under way.

Large-Eddy Simulations

Test cloud fields were created using the 3D, finite-difference flow-solver described by Stevens et al. 1999. This code has been thoroughly evaluated in a number of intercomparisons, (e.g., Bretherton et al. 1997, and Stevens et al. 2001) and provides a state-of-the-art representation of the cloud-topped atmospheric boundary layer. The configuration used here had a 100 x 100 x 110 element grid with 66.66 m x 66.66 m x 40.00 m spacing.

The base cumulus scenario was drawn from case 6 of the Global Energy and Water Cycle Experiment (GEWEX) Cloud System Study Working Group 1. This case simulates a continental boundary layer forced by the diurnal cycle. The initial atmospheric state, illustrated in Figure 1, is based on

measurements made at the Atmospheric Radiation Measurement (ARM) Program Southern Great Plains (SGP) site on June 21, 1997. Radiative and large-scale advective tendencies over time are also derived from observations. The imposed conditions produce radiatively forced development of shallow cumulus, with weak large-scale forcing. The simulations began at 5:30 local time and were run out 12 hours with a base time step of 1.0 to 1.5 s, depending on stability conditions. Model outputs, such as 3D mixing ratio fields, were saved every 15 min after clouds began to form.

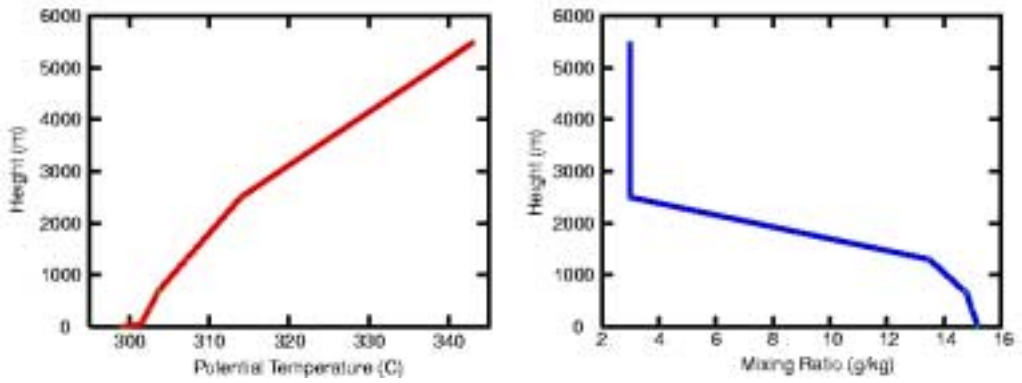

Figure 1. Initial sounding used for the large-eddy simulations.

Simulations run to date are summarized in Table 1. A variety of forcings were imposed to assess the impact of environmental conditions on cloud field structure. Thus far, initial wind speeds and shear profiles, amounts of available water vapor, and the magnitude of surface fluxes have been varied. Examples of the simulated cloud fields appear in Figure 2. Horizontal anisotropy is most evident in run SGPSU10, which includes significant vertical shear in the zonal wind.

Table 1. Summary of simulation cases. Winds and water vapor variations are imposed as initial conditions while surface fluxes are specified for all run times. Wind directions are given using the meteorological convention.

Case	Steady wind	Vertical wind shear	Mean wind in cloud	Other conditions
SGPUO	--	--	--	--
SGPU5	5 ms^{-1} @270°	--	10 ms^{-1} @270°	--
SGPU10	10 ms^{-1} @270°	--	10 ms^{-1} @270°	--
SGPU15	15 ms^{-1} @270°	--	15 ms^{-1} @270°	--
SGPU20	20 ms^{-1} @270°	--	20 ms^{-1} @270°	--
SGPBLW010	10 ms^{-1} @270°	--	10 ms^{-1} @270°	+10% avail. water in BL
SGPU5	--	2 $ms^{1}km^{1}$ @270°	2.4 ms^{1} @270°	--
SGPSU10	--	4 $ms^{-1}km^{-1}$ @270°	4.8 ms^{-1} @270°	--
SGPSV5	10 ms^{-1} @270°	2 $ms^{-1}km^{-1}$ @180°	10.6 ms^{-1} @250°	--
SGPSV10	10 ms^{-1} @270°	4 $ms^{-1}km^{-1}$ @180°	12.3 ms^{-1} @235°	--
SGPF50	10 ms^{-1} @270°	--	10 ms^{-1} @270°	Surface fluxes at 50%
SGPF150	10 ms^{1} @270°	--	10 ms^{1} @270°	Surface fluxes at 150%

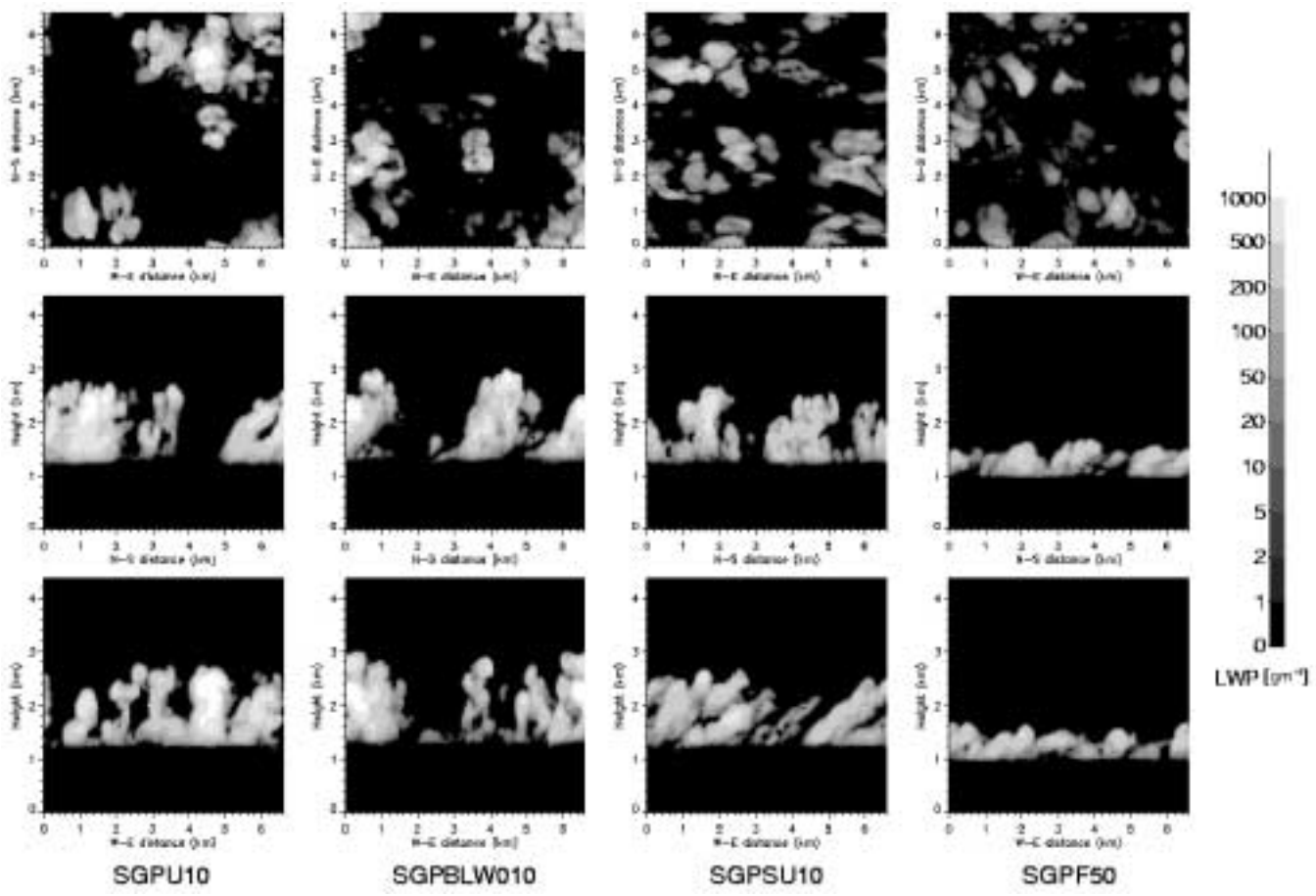

Figure 2. Sample cloud fields from four simulations. Snapshots of integrated liquid water content are shown from the top, west, and south. All images are for 36,000 s into the model run.

While this version of the large-eddy simulation (LES) model includes only a bulk liquid water parameterization and prescribed radiative surface fluxes, we plan to carry out additional simulations using explicit microphysics and a two-stream radiation scheme. This will allow us to evaluate the effect of drizzle, cloud condensation nucleus (CCN) concentrations, ice processes, and radiational heating/ cooling on the development of cloud structure. Independent realizations of a given process, created by using different random potential temperature perturbations to initiate convection in otherwise identical runs, will be used to improve confidence in the results.

Anisotropy Calculations for Model Fields

The second-order anisotropy parameter is used to characterize the structure of two-dimensional (2D) fields. To calculate this parameter, the 2D power spectrum of the field is divided into octave spatial-frequency bands, as shown in Figure 3. (Spatial frequency increases from the center of the spectrum out.) The complex-valued second-order anisotropy parameter, A, is defined for each band according to

$$M_{0,\eta} = \int_{k_n}^{k_n} \int_0^{2\pi} S(k, \phi)\, d\phi\, dk$$

$$M_{c,n} = \int_{k_{n-1}}^{K_n} \int_0^{2\pi} S(k, \phi) \cos(2\phi)\, d\phi\, dk$$

$$M_{s,n} = \int_{k_{n-1}}^{k_n} \int_0^{2\pi} S(k, \phi) \sin(2\phi)\, d\phi\, dk$$

$$|A_n| \equiv \frac{\sqrt{M_{c,n}^2 + M_{s,n}^2}}{M_{0,n}}$$

$$\angle(A_n) \equiv \frac{1}{2} \tan^{-1}\left(\frac{M_{s,n}}{M_{c,n}}\right)$$

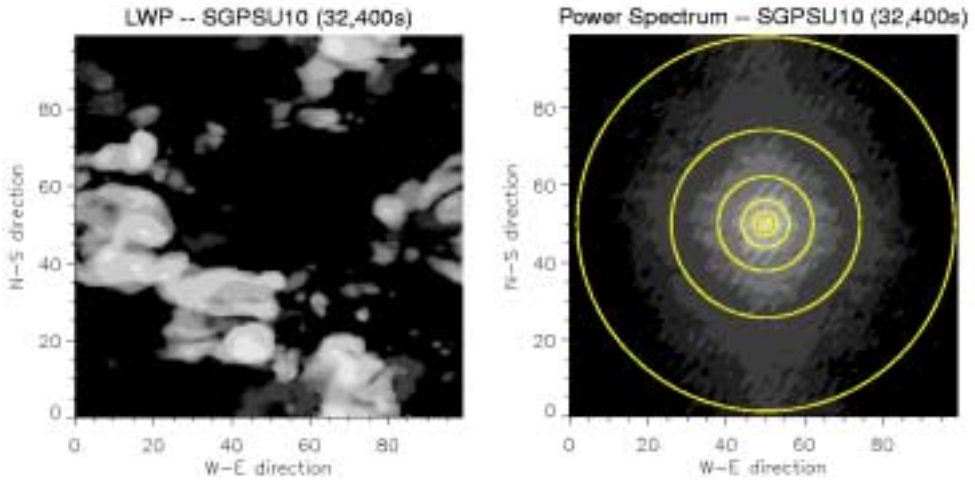

Figure 3. Calculation geometry for the anisotropy parameter. A representative liquid water path (LWP) field from simulation SGPSU10 is shown on the left and its power spectrum appears to the right. The boundaries of the spatial frequency octave bands are indicated on the power spectrum.

The amplitude of the anisotropy parameter indicates the degree to which the field has a preferred orientation and the phase angle specifies the direction of orientation.

The degree of anisotropy in the simulated cloud fields was analyzed using the anisotropy parameter. For each run, the anisotropy parameter was calculated from the average power spectrum of the LWP fields from all scenes with a cloud fraction between 20 and 35 percent. Results for the four example runs shown in Figure 2 are given in Table 2. Because power spectra of real data are conjugate symmetric, all the angles fall within two quadrants. (-90[°] and +90[°] are equivalent, since both are oriented along the zonal direction.) Note that the probability of getting a high amplitude by random chance decreases with an increasing number of sample points, i.e., with increasing spatial frequency. The case with a strong zonal wind shear (SGPSU10) has consistently high anisotropy at angles close to the wind direction.

Table 2. Anisotropy parameter values for four simulations. Each result is for the average of several LWP power spectra from various simulation output times, as described in the text. Spatial frequency (wavelength) increases (decreases) from left to right.

		Spatial-Frequency Band					
Case	**Term**	**(DC) to $(3200\ m)^{-1}$**	**$(3200\ m)^{-1}$ to $(1600\ m)^{-1}$**	**$(1600\ m)^{-1}$ to $(800\ m)^{-1}$**	**$(800\ m)^{-1}$ to $(400\ m)^{-1}$**	**$(400\ m)^{-1}$ to $(200\ m)^{-1}$**	**$(200\ m)^{-1}$ to $(100\ m)^{-1}$**
SGPU10	|A|	0.107	0.115	0.146	0.189	0.027	0.031
	∠(A)	-86.1	-64.8	4.6	0.68	-0.84	82.7
SGPBLW010	|A|	0.087	0.131	0.028	0.055	0.055	0.050
	∠(A)	-22.6	-86.5	-88.7	55.3	44.1	51.0
SGPSU10	|A|	0.171	0.152	0.052	0.170	0.300	0.419
	∠(A)	57.0	69.6	84.5	79.5	88.1	88.4
SGPF50	|A|	0.068	0.044	0.062	0.177	0.227	0.176
	∠(A)	-18.4	-14.2	41.9	31.0	14.9	12.42

Radiative Transfer Calculations

The radiative effect of cloud field anisotropy is studied by importing 3D LES liquid water content fields into a standard 3D Monte Carlo radiative transfer program. The structure of the resulting fluxes, radiances, or atmospheric heating rates is then analyzed using the anisotropy parameter explained above. The level of anisotropy is found to vary among the different radiative fields computed for an individual cloud scene.

Example monochromatic results at 0.67 μm are shown in Figure 4 for the LES run SGP10 scene at 29,700 s. (This field is also being used in Phase II of the Intercomparison of 3D Radiation Codes or I3RC.) The expected feature broadening is evident in the top of atmosphere (TOA) reflectance fields, while high resolution is maintained for the radiances. Shadowing is obvious in the radiance field for a solar zenith angle (SZA) of 60[°], but only faintly visible in the corresponding reflectance field.

The second order anisotropy parameter was calculated for these fields. The results in Table 3 indicate that the radiative fields are substantially more anisotropic in the low-and mid-range spatial frequencies than the original LWP field. This may be due to the nonlinear conversion of LWP to albedo in addition to feature broadening. The nadir radiances for the SZA of 60[°] are particularly anisotropic, which is not unexpected given that side illumination causes an apparent narrowing of cloud structures in the solar azimuthal direction.

Future Work

Future efforts will focus on extending this analysis to a range of representative cumulus and stratocumulus LES cloud fields covering a wide variety of simulation conditions.

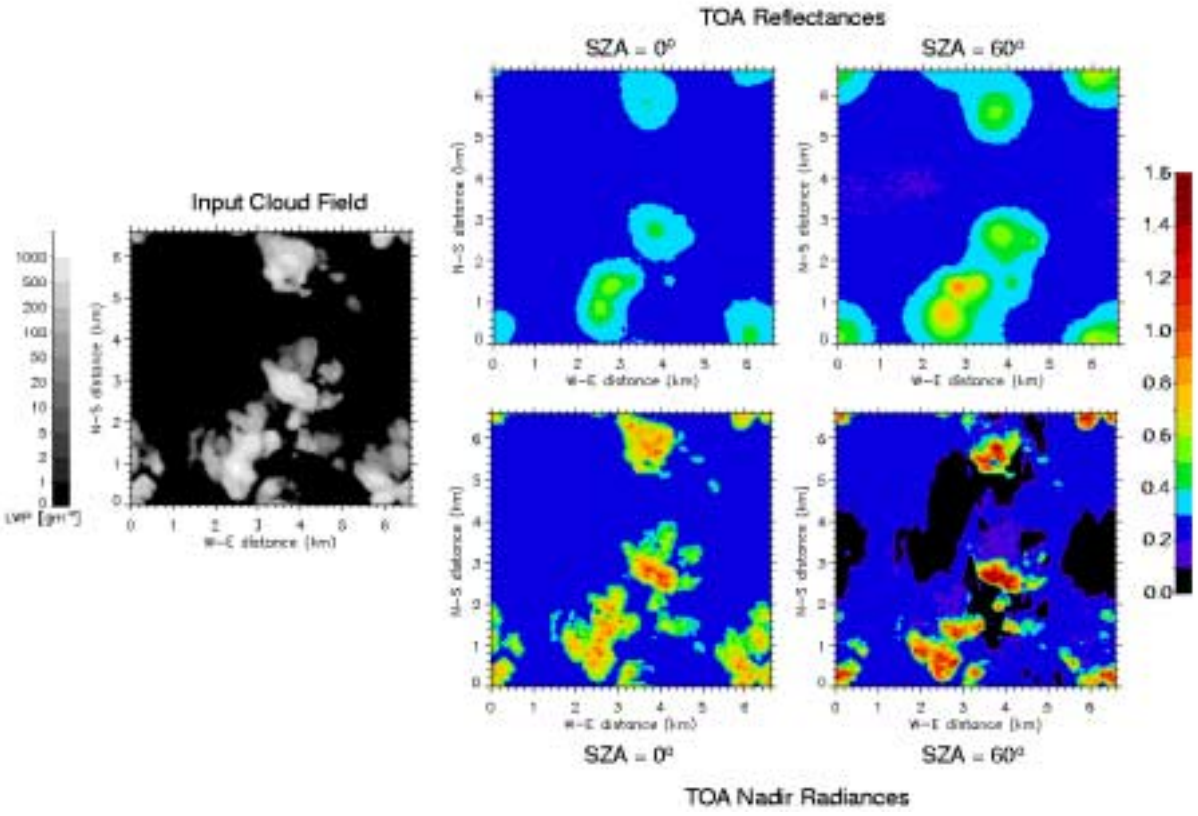

Figure 4. Radiative transfer calculation results. The input cloud field is shown to the left in terms of its LWP. The output radiances and fluxes at the TOA, taken to be 30 km above the surface, are shown in the panels to the right for SZA of 0[°] and 60[°].

Table 3. Anisotropy parameter values for Monte Carlo radiation fields.

Field	Term	Spatial-Frequency Band: (DC) to $(3200\ m)^{-1}$	$(3200\ m)^{-1}$ to $(1600\ m)^{-1}$	$(1600\ m)^{-1}$ to $(800\ m)^{-1}$	$(800\ m)^{-1}$ to $(400\ m)^{-1}$	$(400\ m)^{-1}$ to $(200\ m)^{-1}$	$(200\ m)^{-1}$ to $(100\ m)^{-1}$
LWP	|A|	0.139	0.18	0.102	0.080	0.118	0.057
	∠(A)	-59.3	-12.6	-9.2	13.3	36.7	-89.1
Reflectance SZA = 0°	|A|	0.277	0.303	0.221	0.182	0.141	0.018
	∠(A)	-81.9	-2.8	-31.9	-44.8	8.5	41.0
Reflectance SZA = 60°	|A|	0.428	0.298	0.287	0.177	0.288	0.014
	∠(A)	-80.1	-21.9	-51.1	89.8	37.4	59.4
Radiance SZA = 0°	|A|	0.358	0.239	0.164	0.108	0.135	0.018
	∠(A)	-83.5	4.14	23.3	11.6	28.7	17.9
Radiance SZA - 60°	|A|	0.722	0.358	0.220	0.122	0.157	0.036
	∠(A)	-81.4	24.6	-80.3	68.9	59.9	47.1

Corresponding Author

L. M. Hinkelman, laura@essc.psu.edu, (814) 863-5375

References

Bretherton, C. S., et al., 1997: An intercomparison of radiatively driven entrainment and turbulence in a smoke cloud, as simulated by different numerical models. *QJRMS*., **125**, 391-423.

Stevens, B., C. -H. Moeng, and P. P. Sullivan, 1999: Large-eddy simulations of radiatively driven convection: Sensitivities to the representation of small scales. *JAS*, **56**(23):3963-3984.

Stevens, B., et al., 2001: Trade-cumuli under a strong inversion. *JAS*, accepted for publication.